ACS APPLIED MATERIALS & INTERFACES

Research Article

www.acsami.org

Multifunctional White-Light-Emitting Metal–Organic Gels with a Sensing Ability of Nitrobenzene

Sandipan Roy,[†] Ajit K. Katiyar,[‡] Suvra Prakash Mondal,[‡] Samit K. Ray,[‡] and Kumar Biradha*[,†]

[†]Department of Chemistry and [‡]Department of Physics and Meteorology, Indian Institute of Technology, Kharagpur 721302, India

Supporting Information

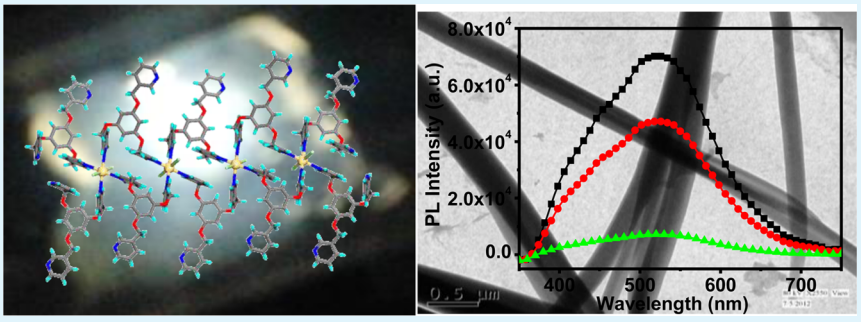

ABSTRACT: In this study, three novel luminescent nanofibrous metal–organic gels (MOGs) have been synthesized by the reaction of 1,3,5-tris(3-pyridylmethoxyl)benzene (**L**) with chloride salts of Cd(II), Hg(II), and Cu(II). The metal–ligand coordination, intermolecular $\pi-\pi$ stacking and several other weak interactions found to play an important role in the formation of nanofibrous materials. The gel materials are characterized by rheology, diffuse reflectance spectra and various microscopic techniques such as TEM, FESEM, and AFM. The gels MOG-1 and MOG-2 were found to exhibit significant white photoluminescence, whereas the MOG-3 exhbits green emission upon excitation at 325 nm. Furthermore, the MOG-1 has shown its application as a chemosensor for the remarkable detection of nitroaromatics such as nitrobenzene (NB), 2,4-dinitrophenol (DNP). The significant quenching response for NB and DNP is attributed to the strong charge-transfer interactions between the electron-deficient aromatic ring of NB and the electron rich aromatic group of **L** in MOG-1. The crystal structure of Cd(II) complex of **L** reveals the formation one-dimensional network which contains strong $\pi-\pi$ interactions within and between the networks and these strong $\pi-\pi$ interactions generate the free charge carrier in all these nanofibrous gels.

KEYWORDS: *white photoluminescence, semiconductivity, charge carrier, nanofiber, metal–organic gels, chemosensor*

INTRODUCTION

The ever increasing demand for miniaturization and high speed technologies urge researchers to find new materials that are capable of producing more sophisticated and compact optical devices. In this regard, the supramolecular self-assembly process (bottom-up approach) of small molecules offers a great promise because of their modular nature and emerged as a powerful technique for the design of functional nanostructure materials.[1−6] The properties of these materials depend not only on chemical nature and composition of the components, but also hugely on their structure, shape, size, spatial arrangements and morphologies. In particular, nanofibers have great prospects for designing nanosized optoelectronic devices.[7−14] The process of gelation, which occurs through self-assembly of one or two chemical components, is one of the interesting methodologies to produce nanofibers. In the gels, the fibers form network structures, through weak interfibril interactions, that trap and immobilize huge amount of solvents.

The nanofibrous gels formed by the low-molecular-mass organic gelators (LMOGs) were shown to have wide range of applications such as drug delivery, sensors, conducting nanowires, light-emitting diodes, and stimuli-responsive opto-electronic devices.[15−27] Very recently, they were also shown to be of utility for white-light-emitting property.[28−33] The white light-emitting materials are of importance because of their solid-state lighting applications such as phosphor lamps and white-light-emitting diodes (WLEDs).[34−37] Generally, white light is generated by the combination of blue, green, and red emissions in required intensities that cover the wavelength from 400 to 700 nm. In addition, white-light-emitting crystalline materials based on metal–organic frameworks (MOFs) or coordination polymers (CPs) have been reported recently.[38−41] Further, electrospun polymer-based nanofibers have shown to exhibit white-light emission.[42] However, white-light-emitting metal–organic gels (MOGs) have not been reported so far, although recent studies on the optical and electroluminescence properties of nanofibrous gels of coordination complexes or polymers have been explored by the groups of Gunnlaugsson, MacLachlan, Rodríguez, Strassert, Vittal, and Yam.[43−48] Despite of several reports on photo physical studies of metal–organic

Received: April 10, 2014
Accepted: July 1, 2014
Published: July 1, 2014

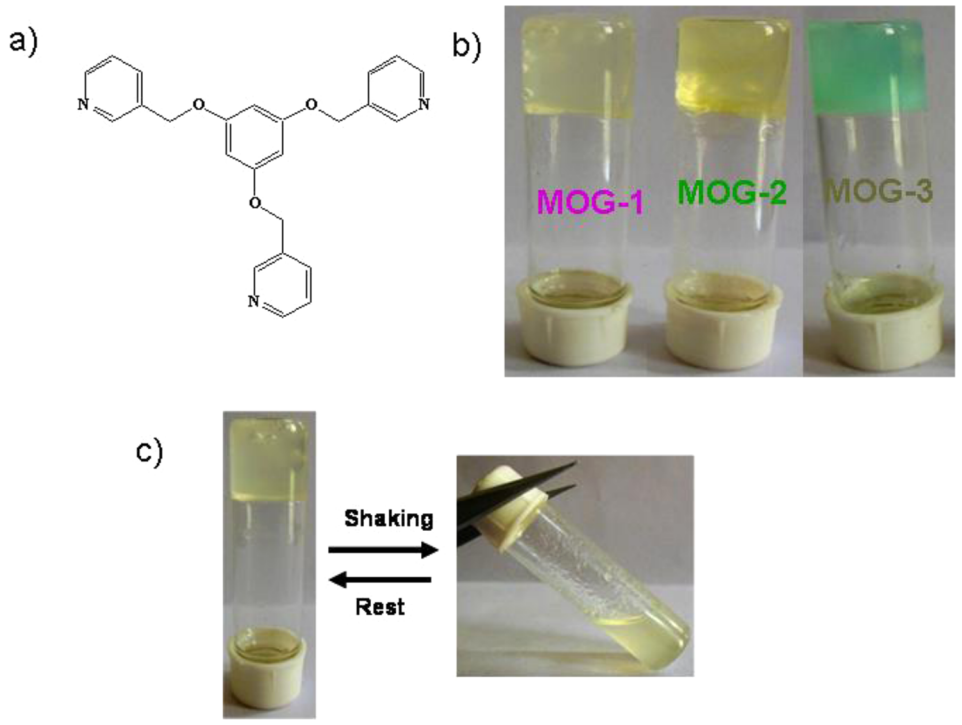

Figure 1. (a) Molecular structure of 1,3,5-tris(3-pyridylmethoxyl)benzene (**L**). (b) Photographs of the inverted vials of MOG-1, MOG-2, and MOG-3. (c) Illustration for the mechano responsive (thixotropic) behavior.

gels (MOGs), to date very little has been explored on their conducting nature.[49] Furthermore, very few studies have shown the utility of MOGs as chemosensors.[50,51] To the best of our knowledge, no metal−organic gel has been shown to exhibit the combination of white light-emission and chemosensor properties.

Here we report one such interesting nanofibrous MOGs of a ligand, namely 1,3,5-tris(3-pyridylmethoxyl)benzene (**L**), that exhibits remarkable white luminescence and sensing ability of nitrobenzene. Further, the properties of the gel are found to depend on the nature of the metal atoms and more importantly the gel material found to exhibit much better properties than the corresponding xerogel. The ligand **L** is of our interest (Figure 1a), as it possesses flexibility in the form of $-OCH_2-$ groups and three-pyridyl groups for coordination and has a possibility to exist in various geometries, for example well-known 3-fold and tripodal geometries. Recently, **L** was shown to form CPs with $ZnCl_2$, $MnCl_2$, and Ag(I) salts.[52,53] Several LMOG's with 3-fold symmetry and flexibility were shown to form organic or hydrogels, but only three such examples were shown to form CP-gels to date.[43,54−56] Therefore, the complexation reactions of **L** were carried out with halide salts of Cd(II), Hg(II), and Cu(II) in anticipation of crystalline materials of CPs. However, under the given conditions these reactions resulted in the formation gels. As we have recently explored MOGs of bis(benzimidazole)-based ligand with metal halides and demonstrated their chemical and mechano-responsive (thixotropic) properties,[57] we aimed to characterize the MOGs of **L** and explore their multifunctional properties such as luminescence, lifetime, chemo-sensing, thixotropy, mechanical strength (rhehology), and gas sorption ability.

EXPERIMENTAL SECTION

General. All commercially available reagents and solvents were used as received. The ligand **L** was synthesized following a procedure reported in literature.[52] Powder XRD data were recorded with a PHILIPS Holland PW-171 difractometer with Cu Kα radiation (λ = 1.54178 Å). The Diffuse reflectance spectra (DRS) of the nanofibers were recorded with a Cary Model 5000 UV−visible−NIR spectrophotometer.

Crystal Structure Determination. The single-crystal data were collected on a Bruker-APEX-II CCD X-ray diffractometer that uses graphite monochromated Mo Kα radiation (λ = 0.71073 Å) at room temperature (293 K) by the hemisphere method. The structure was solved by direct methods and refined by least-squares methods on F^2 using SHELX-97.[58] Non-hydrogen atoms were refined anisotropically and hydrogen atoms were fixed at calculated positions and refined using a riding model.

Field Emission Scanning Electron Microscope (FE-SEM). The morphologies of the xerogel materials were characterized by field emission scanning electron microscope (FESEM, Zeiss, Supra-40) operating at 5−10 Kv. Samples were prepared by dropping the diluted gels on the aluminum foils and then dried by air for 12 h. A thin layer of Au was deposited onto the samples to minimize sample charging before SEM examination.

Transmission Electron Microscopy (TEM). The gel materials were examined by a transmission electron microscope (FEI-TECNAI G2 20S-TWIN, Type-5022/22). Samples were prepared by dropping the diluted gels on the carbon-coated copper grids.

Atomic Force Microscope (AFM). The surface morphologies of the xerogel materials were characterized by atomic force microscopy (Veeco Nanoscope-IV) with tapping mode.

Photoluminescence and Decay Studies. Photoluminescence (PL) measurements were carried out using a He−Cd laser as the excitation source operating at 325 nm with an output power of 50 mW at room temperature. Each gel and xerogel sample (approximately 20 mg) was kept in a quartz cell and then kept in front of the laser for excitation. The emission was then recorded in a wavelength range of 310 to 800 nm using a TRIAX-320 monochromator and Hamamatsu R928 photomultiplier detector. The photoluminescence (PL) lifetime decay measurements were done using an Edinburgh Instruments (Life Spec-II, EPL 405) measurement unit with a 404.4 nm excitation pulse diode laser.

Sampling Procedure of Sensing and Its Recyclability. The solid-state fluorescence quenching of MOG-1 with different nitro-containing analytes was performed by inserting the freshly prepared spin-coated film of MOG-1 into the beaker containing saturated vapor of respective analytes. After 5 min exposure of the film to the saturated vapor of analytes, the film was placed in the sample holder immediately and checked for the fluorescence quenching of the initial film intensity. The observed fluorescence quenching was calculated using the following equation $\eta = (I_0 - I/I_0) \times 100\%$, where I_0 is the initial fluorescence intensity of the MOG-1 film and I is the fluorescence intensity after a period of exposure time. For the recyclability of the sensing process, the film of MOG-1 was treated by dry air flow and again recorded the emission spectrum of that film. The whole process was repeated four times.

Rheological Measurements. For all the gel samples, rheological measurements were carried out on a Bohlin Gemini (Malvern, UK) controlled-stress rheometer using 20 mm diameter parallel plate geometry with a constant tool gap of 200 μm. The gel sample was placed on the lower plate, and a stress amplitude sweep experiment was carried out at a constant frequency at 25 °C to obtain storage or elastic modulus, G', and loss or viscous modulus, G''. The frequency sweep measurements were carried out at a constant stress in the linear viscoelastic range.

Gas Sorption Study. The gas sorption studies were conducted on the dried xerogels of MOGs using a Quantacrome autosorb iQ automated gas sorption analyzer. Generally, 20−25 mg of sample was taken in a 6 mm sample holder without a rod. Prior to the sorption experiment, the samples were employed for degassing at 70 °C for 2 h.

Gel Formation. In a typical gel formation reaction, 10 mg (0.02 mmol/mL) of ligand (**L**) was placed in ten different glass vials, and 0.1−1.0 equiv of metal salt with respect to the ligand concentration was also placed in 10 different glass vials. The ligand (**L**) was dissolved in methanol (1 mL) and metal salt dissolved in water (1 mL) separately. Finally the aqueous solution of metal salt added to the methanolic solution of **L** such that the total volume of the solvent in each vial is 2 mL. The screw capped glass vials were then left at room temperature.

RESULTS AND DISCUSSION

The addition of aqueous solution (1 mL) of metal halides (1 equiv) to the MeOH solution (1 mL) of ligand **L** (6 mg, 1 equiv) resulted in transparent metal−organic gels upon standing under ambient conditions. The MOG-1, MOG-2 and MOG-3 were shown an ability to gelate MeOH−H_2O with minimum gelation concentrations (MGC) of 0.036%, 0.040% and 0.035% (w/v) respectively. In the cases of $CdCl_2$ and $HgCl_2$, the gelation occurs instantly (within 2 to 3 min) to form transparent white (MOG-1) and light yellow colored (MOG-2) gels, respectively. Similar reaction of $CuCl_2$ with **L** resulted in the clear solution which upon standing for two hrs at ambient conditions forms light green colored gel (MOG-3). The formations of gels were confirmed by the inverted vial method and MOGs were found to be stable in capped vials for several months (Figure 1b). The chloride salts of metals were found to be essential for gelation as the use of salts of several other anions such as bromide, nitrate, tetrafluoroborate, perchlorate and acetate not resulted in the formation of gels. Gelation was found to occur not only in MeOH-H_2O, they also found to occur in EtOH-H_2O, propanol-H_2O, CH_3CN-H_2O, MeOH, EtOH, propanol, and butanol. Further, all the three MOGs were found to exhibit thixotropic behavior that is shaking the gel containing vials for few minutes results in the formation of a free-flowing liquid that upon standing for 8−12 h reforms gels (Figure 1c).

The morphologies of the MOGs were investigated by transmission electron microscope (TEM), field emission scanning electron microscope (FESEM) and atomic force microscope (AFM). TEM pictures reveal that all three MOGs exhibit an entangled three-dimensional (3D) network consist of fibers with various widths in several nanometers and lengths of several micrometers. The MOG-1, MOG-2 and MOG-3 exhibit widths of 200−450 nm, 80−400 nm and 80−200 nm respectively (Figure 2). These observations were further

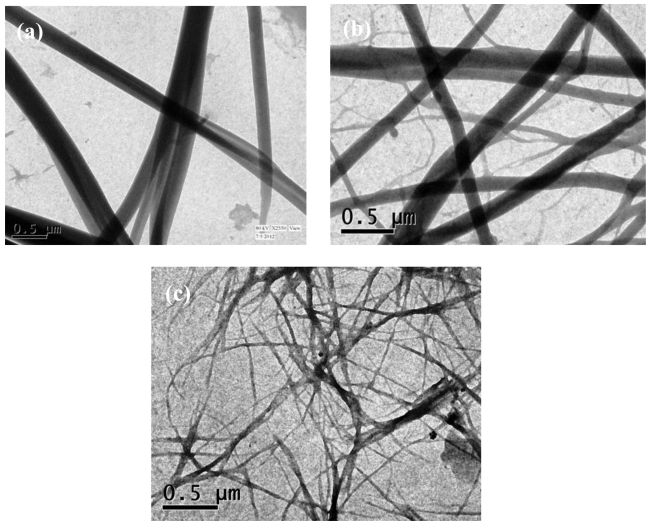

Figure 2. Morphological characterization of metal−organic gels by TEM. (a) Fiber morphology of MOG-1 drop casted on the carbon coated copper grids from MeOH-H_2O, as observed by TEM. (b) TEM micrograph of MOG-2 fibers. (c) TEM micrograph of MOG-3 fibers.

confirmed with FESEM and AFM (see the Supporting Information, Figures S2 and S3). Rheological studies were carried out to understand the mechanical properties of MOGs. The yield stress (σ_y) values of MOG-1, -2, and -3 were found to be 53, 7.9, and 8.3 Pa, respectively (Figure 3a, b and Figures S5 and S6 in the Supporting Information). These values indicate the remarkable firmness of the MOG-1 compared to other two gels as well as many reported metal−organic or coordination gels.[59,60] The microscopic studies suggested that the xerogel materials may exhibit porosity. Therefore, the porosity of the xerogels was explored by conducting N_2 gas sorption. The xerogel of MOG-1 exhibits a N_2-sorption isotherm of type-III, indicating the macroporous nature of the solid (Figure 3c). Further, the xerogel of MOG-1 found to exhibit a total surface area of 19.14 $m^2\ g^{-1}$, total pore volume of 8.61×10^{-3} $cm^3\ g^{-1}$, and N_2 gas uptake capacity of 52.83 $cm^3\ g^{-1}$. These values are comparable with our previously reported coordination based gels.

The flexible ligand **L** is capable of forming CPs of one-, two-, and three-dimensional networks.[52−54] To understand the type of polymeric aggregation present in these current MOGs, several crystallization attempts of gels were carried out with slight alterations in the gelation conditions. In one of such reactions, we are fortunate to obtain single crystals suitable for X-ray diffraction in the case of MOG-1. The method employed here is that the gel was formed in somewhat dilute conditions, that is by adding 1 mL of aqueous solution of $CdCl_2$ (2.8 mg, 1 equiv) to 1.5 mL of MeOH solution of **L** (5 mg, 1 equiv). The gelation occurred immediately and upon standing for 6−7 days resulted in colorless single crystals of complex $\{[Cd_2(\mathbf{L})_2Cl_2].H_2O\}_n$ (**1**). The crystal structure of **1** exhibits $P2/c$ space group and the asymmetric unit contains one unit

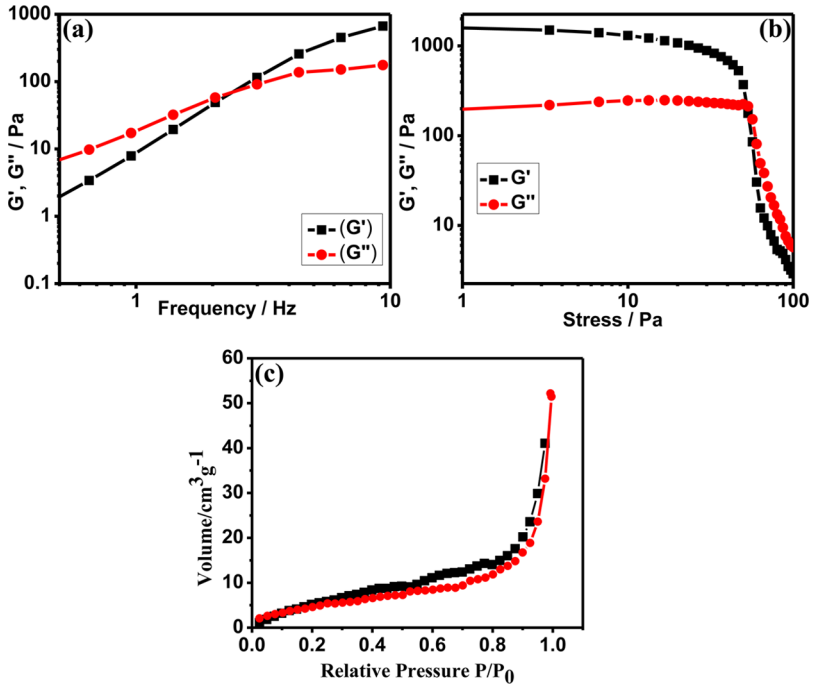

Figure 3. Illustrations for rheological and porous behavior of MOG-1: (a) Variation of storage modulus (G') and loss modulus (G'') with frequency. (b) Variation of G' and G'' with shear stress. (c) N_2 gas sorption isotherm of xerogel of MOG-1.

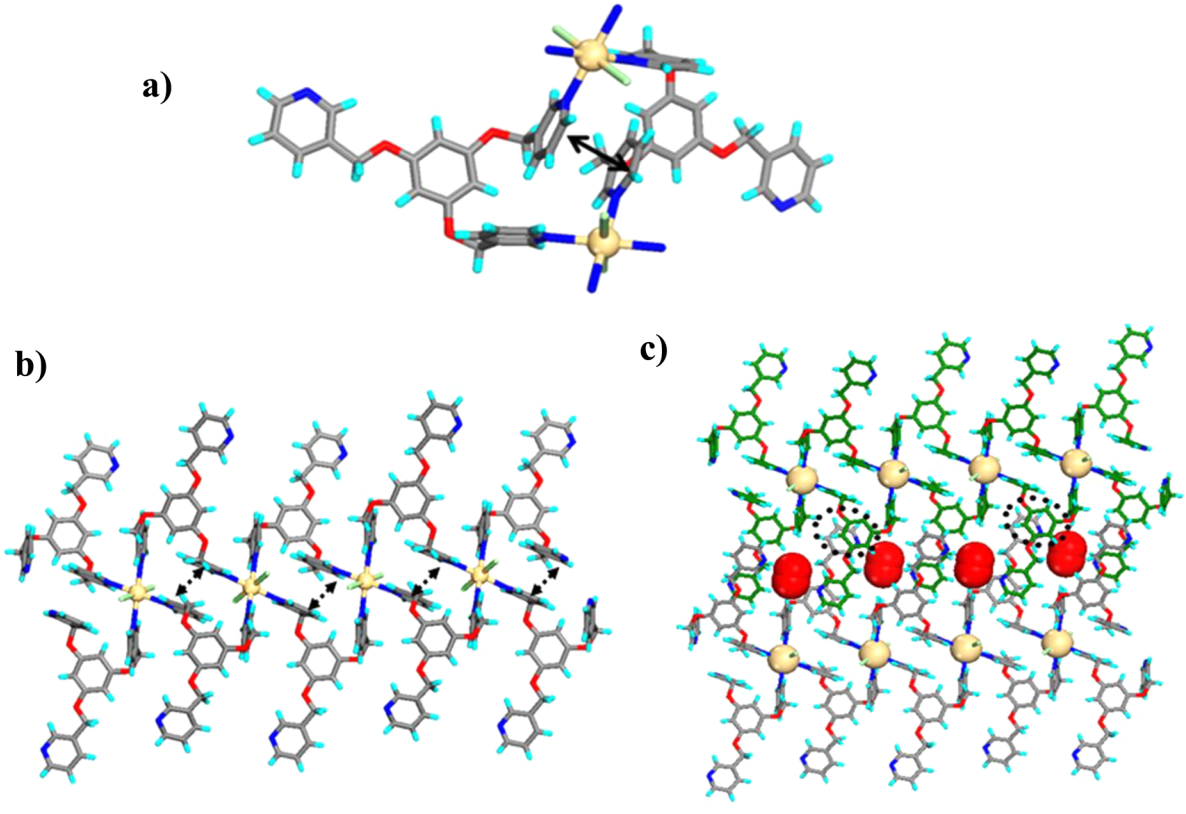

Figure 4. Illustrations for the crystal structure of **1**: (a) Macrocylce of $Cd_2(\mathbf{L})_2$ unit, which results in face-to-face $\pi-\pi$ interaction between the two 3-pyridyl units of **L** with centroid-to-centroid distance of 3.64 Å. (b) One-dimensional network formed by the linking of macrocycles of $Cd_2(\mathbf{L})_2$ units, notice the alignment of uncoordinated 3-pyridyl groups on both sides of the chain. (c) Packing of one-dimensional chains via $\pi-\pi$ interactions (dotted circles) between 3-pyridyl and central C_6-ring, the neighboring chain was colored in green for the sake of clarity.

each of **L**, Cd(II) ion, and Cl^- anion and half a unit of H_2O. The ligand **L** exhibits nonplanar and divergent geometry; only two pyridine groups of **L** were involved in coordination. The Cd(II) exhibits octahedral coordination geometry with four pyridyl groups from different units of **L** at equatorial positions and the two Cl atoms are at the epical positions (Figure 4a).

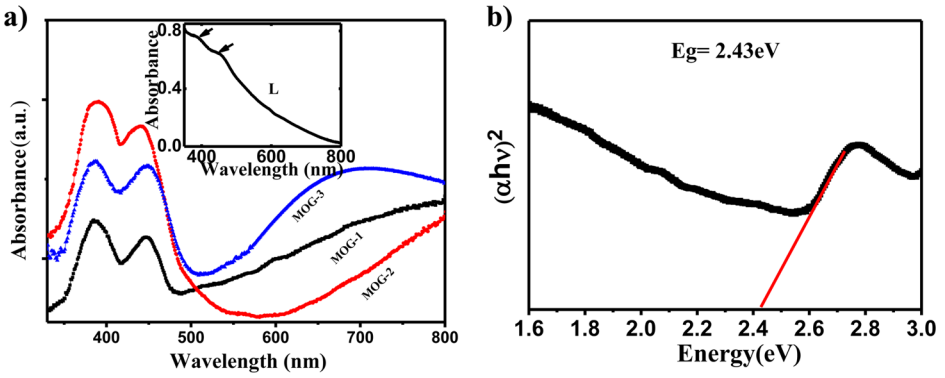

Figure 5. (a) UV–vis diffuse reflectance spectra of MOG-1 (black line), MOG-2 (red line) and MOG-3 (blue line). The inset shows UV–vis DRS of **L**. (b) Plot of $(\alpha h\nu)^2$ vs $h\nu$ of MOG-1 for optical band gap calculation.

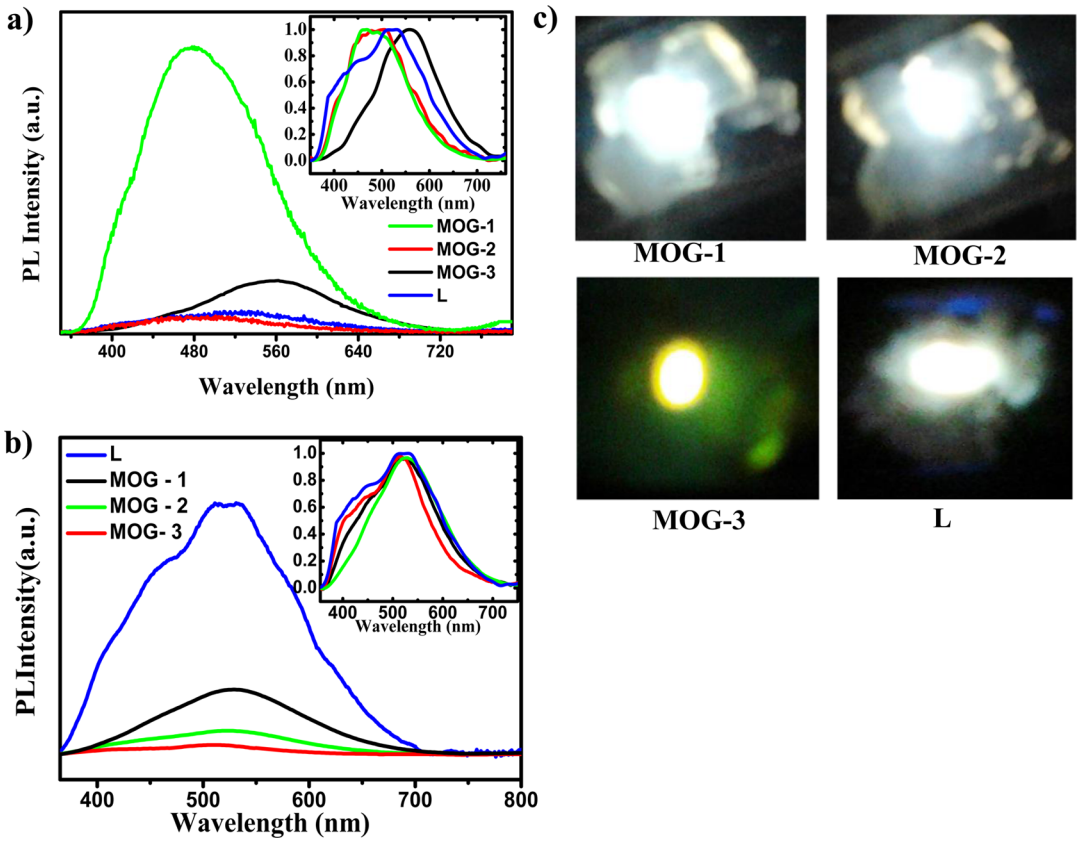

Figure 6. (a) Photoluminescence spectra (PL) of MOG-1 (green line), MOG-2 (red line), MOG-3 (black line), and **L** (blue line). The inset shows the normalized PL spectra of all three MOGs and **L**. (b) PL spectra of xerogels of MOG-1 (black line), MOG-2 (green line), MOG-3 (red line) and **L** (blue line). The inset shows the normalized PL spectra of all three xerogels and **L**. (c) Luminescence photographs of MOG-1, MOG-2, MOG-3, and **L** under the excitation wavelength of 325 nm.

The geometry of the ligand with such coordination environment of Cd(II) results in the formation one-dimensional CP (Figure 4b). In other words, such macrocylces of $Cd_2(\mathbf{L})_2$ units are connected to form a one-dimensional chain with a Cd(II)–Cd(II) distance of 8.29 Å.). Further, within the macrocycles, face-to-face π–π interactions are exhibited between the coordinated 3-pyridyl groups of two units of **L** with a centroid-to-centroid distance of 3.64 Å (Figure 4a). Furthermore, the uncoordinated 3-pyridyl units hang on the both sides of the one-dimensional chain such that they align in opposite directions on both sides. These 3-pyridyl groups form π–π interactions with the central C_6-unit of the adjacent chains (Figure 4c). The powder X-ray diffraction pattern (PXRD) of single crystals of complex **1** and the xerogel of MOG-1 were performed to investigate their molecular packing. The comparison of PXRD pattern of complex **1** with that of xerogel of MOG-1 reveals that xerogel contains crystalline metal–organic components and further it can be conclude that the xerogel of MOG-1 is also constituted by such one-dimensional CPs and packing (see Figure S1 in the Supporting Information).

Because of the existence of π–π interactions, the one-dimensional coordination network and fibrous nature of the material prompted us to investigate its properties such as solid-state UV–vis diffuse reflectance spectra (DRS), photoluminescence, and chemo-sensing. The DRS of the ligand **L**

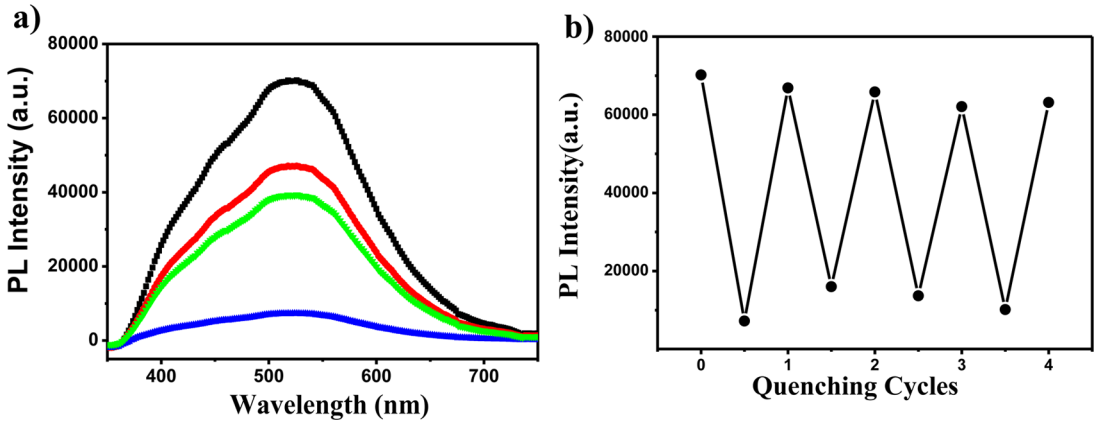

Figure 7. (a) Fluorescence spectra of a spin coated film of MOG-1 before (black line) and after exposure to NM (red line), DNP (green line), and NB (blue line) vapors. (b) Recyclability of sensing of saturated vapor of nitrobenzene (NB) by MOG-1 film.

and MOGs were recorded at room temperature. The ligand **L** shows two weak shoulder absorption bands at 380 and 448 nm. On the other hand, MOGs exhibit two sharp and strong absorption bands in the regions of 360−390 and 448 nm (Figure 5a). The first peak (360−390 nm) is ascribed to typical $\pi \rightarrow \pi^*$ transition and the second one (448 nm) is attributed to the intraligand charge transfer transition. In addition, all three systems (MOG-1−3) are found to exhibit absorption band in the entire visible region including 600−800 nm. This broad entire visible absorption band could be the result of strong intermolecular aromatic π-stacking induced charge transfer transition.[61−63] The optical band gaps were calculated to be 2.43, 2.34, and 2.30 eV for MOG-1−3 respectively. (Figure 5b, see Figure S8 in the Supporting Information). These features further encouraged us to explore their photoluminescence and conducting properties.

The solid-state luminescence for the ligand **L** and MOGs were investigated at room temperature with an excitation wavelength of 325 nm. The free ligand **L** displays a broad, white emission profile with an emission maximum at 522 nm (λ_{ex}= 325 nm). This emission may be attributed to the $\pi-\pi$ interactions between the units of **L**. In MOG-1, this band differs significantly in terms of emission wavelength as well as intensity with respect to **L**. It displays a broad, white emission profile with an emission maximum at 490 nm and the luminescence intensity was enhanced by 14 times with respect to that of **L** (Figure 6a, c). Similarly, MOG-2 also displays a broad, white emission profile with an emission maximum at 490 nm. In contrast, MOG-3 shows a green emission with an emission maximum at 528 nm. However, in both cases, no significant change in emission intensity with respect to that of **L** was observed. Further, it is interesting to note here that all the xerogels of MOG-1,-2 and −3 exhibited emission band at 522 nm, similar to **L**, with considerable drop in the intensity compared to that of their gel state (Figure 6b). The quenching of this emission intensity in the xerogels could be due to the generation of high concentration of charge carriers as a result of close packing and therefore better $\pi-\pi$ interactions in xerogel, as observed in the crystal structure of **1**. These results imply that the emission profiles of MOGs differ significantly with those of **L**, both in terms of intensity and wavelength. Further, the time-resolved photoluminescence measurements for all the MOGs were carried out at emission wavelength of 550 nm. The fluorescence decay of MOG-1 was fitted with a single exponential component, yielding a lifetime of 3.46 ns (see Figure S4 in the Supporting Information), which indicates that this emission is fluorescence. In contrast, the fluorescence lifetimes for MOG-2 and MOG-3 were found to be 2.35 and 1.84 ns, respectively. This decay study clearly demonstrates that MOG-1 exhibits longer lifetime compared to MOG-2 and -3. This result reflects the fact that MOG-1 in the aggregate state is more rigid and restricts the rotational and vibrational motions of the molecules. Therefore, the limited molecular motions decrease the nonradiative relaxation process; which leads to a longer lifetime and fluorescence enhancement.[64]

To investigate the direct application of MOG-1 as an effective chemosensor toward nitro-explosives, we have prepared spin-coated film of MOG-1. The solid-state fluorescence quenching experiment of the sensing film of MOG-1 was performed upon few minute exposures to saturated vapors of nitro-containing aromatic and nonaromatic molecules such as nitrobenzene (NB), 2,4-dinitrophenol (DNP) and nitromethane (NM). Nearly 90% quenching efficiency was observed upon 5 min exposure of the MOG-1 film to saturated vapor of nitrobenzene (Figure 7a). This result is attributed to the strong charge-transfer interactions between the electron-deficient aromatic ring of NB and the electron rich aromatic surfaces of MOG-1 film. To the best of our knowledge, this is the highest quenching effect of nitrobenzene compared to reported nitrobenzene sensors based on MOF or MOG in the solid state.[65−67] It is interesting to note here that recently an electrospun fluorescent nanofibrous film was found to exhibit 93% quenching efficiency because of the sensing of the vapors of 2,4-dinitro toluene.[68] Further, the MOG-1-based sensor was found to be recyclable (Figure 7b). For example, the film of MOG-1 was significantly retained nearly 91% initial fluorescence intensity even after four cycles. Further, the spin-coated film of MOG-1 also exhibited nearly 54% reduction in the initial fluorescence intensity upon 5 min exposure of the film to saturated vapor of 2,4-dinitrophenol (DNP). The higher quenching efficiency of the MOG-1 film by NB over 2,4-DNP might be due to the relatively higher vapor pressure of NB. Interestingly, nonaromatic analyte such as nitromethane (NM) showed a lower quenching response (33%) than other two nitro-aromatic analytes. This lower quenching response of NM is due to the lack of $\pi-\pi$ interactions as it has no electron-deficient aromatic ring.

Further, the exposure of the film of MOG-1 to the saturated vapors of other aromatic compounds like benzene (BN), ethylbenzene(EBN) and toluene (TN) results in no considerable

change of initial fluorescence intensity (see Figure S7 in the Supporting Information). Hence, this spin-coated film of MOG-1 exhibits highly selective quenching response toward the electron deficient aromatics over the electron rich aromatics.

CONCLUSIONS

In summary, we have successfully developed novel luminescent metal−organic gels by simply mixing the chloride salts of Cd(II), Hg(II) and Cu(II) with ligand **L**. Notably, MOG-1, MOG-2 and **L** were found to exhibit white-light emission, whereas an intense green emission was observed in case of MOG-3. In particular, MOG-1 was found to exhibit more than 14 times higher-intensity photoluminescence than **L** and the other two MOGs. The characterizations of the gel materials with various microscopic techniques reveal their nanofibrous nature with extended network structures. The crystal structure of $CdCl_2$ complex of **L** indicates the formation of one-dimensional polymeric network in which the intermolecular aromatic $\pi-\pi$ interactions significantly contribute, within as well as between the networks, for self-assembly process and also these interactions are responsible for the observed physical properties. Further, the MOG-1 was demonstrated as an effective chemosensor for nitroaromatics and also found to exhibit selective response to electron-deficient aromatics over electron-rich aromatics.

ASSOCIATED CONTENT

Supporting Information

Crystallographic table; powder XRD profiles; FESEM and AFM images of MOG-1, MOG-2, MOG-3; time-resolved fluorescence decay; rheological data of MOG-2 and MOG-3. This material is available free of charge via the Internet at http://pubs.acs.org.

AUTHOR INFORMATION

Corresponding Author

*E-mail: kbiradha@chem.iitkgp.ernet.in.Tel: +91- 3222-283346. Fax: +91-3222-282252.

Notes

The authors declare no competing financial interest.

ACKNOWLEDGMENTS

We gratefully acknowledge financial support from DST and DST-FIST for the single-crystal X-ray facility. S.R. thanks IIT-KGP for a research fellowship.

REFERENCES

(1) Lehn, J.-M. Toward Self-Organization and Complex Matter. *Science* **2002**, *295*, 2400−2403.
(2) Aida, T.; Meijer, E. W.; Stupp, S. I. Functional Supramolecular Polymers. *Science* **2012**, *335*, 813−817.
(3) Ruben, M.; Rojo, J.; Romero-Salguero, F. J.; Uppadine, L. H.; Lehn, J.-M. Grid-Type Metal Ion Architectures: Functional Metallosupramolecular Arrays. *Angew. Chem., Int. Ed.* **2004**, *43*, 3644−3662.
(4) Badjić, J. D.; Balzani, V.; Credi, A.; Silvi, S.; Stoddart, J. F. A Molecular Elevator. *Science* **2004**, *303*, 1845−1849.
(5) O'Keeffe, M.; Yaghi, O. M. Deconstructing the Crystal Structures of Metal−Organic Frameworks and Related Materials into Their Underlying Nets. *Chem. Rev.* **2012**, *112*, 675−702.
(6) Capito, R. M.; Azevedo, H. S.; Velichko, Y. S.; Mata, A.; Stupp, S. I. Self-Assembly of Large and Small Molecules into Hierarchically Ordered Sacs and Membranes. *Science* **2008**, *319*, 1812−1816.
(7) Wang, Y.; Tran, H. D.; Liao, L.; Duan, X.; Kaner, R. B. Nanoscale Morphology, Dimensional Control, and Electrical Properties of Oligoanilines. *J. Am. Chem. Soc.* **2010**, *132*, 10365−10373.
(8) Duan, X.; Huang, Y.; Cui, Y.; Wang, J.; Lieber, C. M. Indium Phosphide Nanowires as Building Blocks for Nanoscale Electronic and Optoelectronic Devices. *Nature* **2001**, *409*, 66−69.
(9) Durham, J. W.; Zhu, Y. Fabrication of Functional Nanowire Devices on Unconventional Substrates Using Strain-Release Assembly. *ACS Appl. Mater. Interfaces* **2013**, *5*, 256−261.
(10) Babel, A.; Li, D.; Xia, Y.; Jenekhe, S. A. Electrospun Nanofibers of Blends of Conjugated Polymers: Morphology, Optical Properties, and Field-Effect Transistors. *Macromolecules* **2005**, *38*, 4705−4711.
(11) Camposeo, A.; Persano, L.; Pisignano, D. Light-Emitting Electrospun Nanofibers for Nanophotonics and Optoelectronics. *Macromol. Mater. Eng.* **2013**, *298*, 487−503.
(12) Kiriya, D.; Kawano, R.; Onoe, H.; Takeuchi, S. Microfluidic Control of the Internal Morphology in Nanofiber-Based Macroscopic Cables. *Angew. Chem., Int. Ed.* **2012**, *51*, 7942−7947.
(13) Bedford, N. M.; Dickerson, M. B.; Drummy, L. F.; Koerner, H.; Singh, K. M.; Vasudev, M. C.; Durstock, M. F.; Naik, R. R.; Steckl, A. J. Nanofiber-Based Bulk-Heterojunction Organic Solar Cells Using Coaxial Electrospinning. *Adv. Energy Mater.* **2012**, *2*, 1136−1144.
(14) Zhou, W.; Yu, H. Conductive Hybrid Nanofibers Self-Assembled with Three Different Amphiphilic Salts. *ACS Appl. Mater. Interfaces* **2012**, *4*, 2154−2159.
(15) Vintiloiu, A.; Leroux, J.-C. Organogels and Their Use in Drug Delivery-A Review. *J. Controlled Release* **2008**, *125*, 179−192.
(16) Dufresne, M.-H.; Marouf, E.; Kränzlin, Y.; Gauthier, M. A.; Leroux, J.-C. Lipase is Essential for the Study of *in Vitro* Release Kinetics from Organogels. *Mol. Pharm.* **2012**, *9*, 1803−1811.
(17) Prasanthkumar, S.; Saeki, A.; Seki, S.; Ajayaghosh, A. Solution Phase Epitaxial Self-Assembly and High Charge-Carrier Mobility Nanofibers of Semiconducting Molecular Gelators. *J. Am. Chem. Soc.* **2010**, *132*, 8866−8867.
(18) Prasanthkumar, S.; Gopal, A.; Ajayaghosh, A. Self-Assembly of Thienylenevinylene Molecular Wires to Semiconducting Gels with Doped Metallic Conductivity. *J. Am. Chem. Soc.* **2010**, *132*, 13206−13207.
(19) Li, X.-Q.; Stepanenko, V.; Chen, Z.; Prins, P.; Siebbelesb, L. D. A.; Würthner, F. Functional Organogels From Highly Efficient Organogelator Based on Perylene Bisimide Semiconductor. *Chem. Commun.* **2006**, 3871−3873.
(20) Luis, J. P.; Laukhin, V.; Pino, Á. P.; Gancedo, J. V.; Rovira, C.; Laukhina, E.; Amabilino, D. B. Supramolecular Conducting Nanowires from Organogels. *Angew. Chem., Int. Ed.* **2007**, *46*, 238−241.
(21) Mukhopadhyay, P.; Iwashita, Y.; Shirakawa, M.; Kawano, S.-i.; Fujita, N.; Shinkai, S. Spontaneous Colorimetric Sensing of the Positional Isomers of Dihydroxynaphthalene in a 1D Organogel Matrix. *Angew. Chem., Int. Ed.* **2006**, *45*, 1592−1595.
(22) Kartha, K. K.; Mukhopadhyay, R. D.; Ajayaghosh, A. Supramolecular Gels and Functional Materials Research in India. *Chimia* **2013**, *67*, 51−63.
(23) Babu, S. S.; Praveen, V. K.; Ajayaghosh, A. Functional π-Gelators and Their Applications. *Chem. Rev.* **2014**, *114*, 1973−2129.
(24) Bairi, P.; Roy, B.; Nandi, A. K. A Light Harvesting Bi-Component Hydrogel with a Riboflavin Acceptor. *Chem. Commun.* **2012**, *48*, 10850−10852.
(25) Krieg, E.; Shirman, E.; Weissman, H.; Shimoni, E.; Wolf, S. G.; Pinkas, I.; Rybtchinski, B. Supramolecular Gel Based on a Perylene Diimide Dye: Multiple Stimuli Responsiveness, Robustness, and Photofunction. *J. Am. Chem. Soc.* **2009**, *131*, 14365−14373.
(26) Kartha, K. K.; Babu, S. S.; Srinivasan, S.; Ajayaghosh, A. Attogram Sensing of Trinitrotoluene with a Self-Assembled Molecular Gelator. *J. Am. Chem. Soc.* **2012**, *134*, 4834−4841.
(27) Sajisha, V. S.; Maitra, U. Multi-Component, Self-Assembled, Functional Soft Materials. *Chimia* **2013**, *67*, 44−50.
(28) Vijayakumar, C.; Praveen, V. k.; Ajayaghosh, A. RGB Emission through Controlled Donor Self-Assembly and Modulation of

Excitation Energy Transfer: A Novel Strategy to White-Light-Emitting Organogels. *Adv. Mater.* **2009**, *21*, 2059−2063.
(29) Bairi, P.; Roy, B.; Chakraborty, P.; Nandi, A. K. Co-assembled White-Light-Emitting Hydrogel of Melamine. *ACS Appl. Mater. Interfaces* **2013**, *5*, 5478−5485.
(30) Rao, K. V.; Datta, K. K. R.; Eswaramoorthy, M.; George, S. J. Highly Pure Solid-State White-Light Emission from Solution-Processable Soft-Hybrids. *Adv. Mater.* **2013**, *25*, 1713−1718.
(31) Molla, M. R.; Ghosh, S. Hydrogen-Bonding-Mediated J-Aggregation And White-Light Emission from a Remarkably Simple, Single-Component, Naphthalenediimide Chromophore. *Chem.—Eur. J.* **2012**, *18*, 1290−1294.
(32) Abbel, R.; van der Weegen, R.; Pisula, W.; Surin, M.; Leclère, P.; Lazzaroni, R.; Meijer, E. W.; Schenning, A. P. H. J. Multicolour Self-Assembled Fluorene Co-Oligomers: From Molecules to the Solid State via White-Light-Emitting Organogels. *Chem.—Eur. J.* **2009**, *15*, 9737−9746.
(33) Maiti, D. K.; Banerjee, A. A Peptide Based Two Component White Light Emitting System. *Chem. Commun.* **2013**, *49*, 6909−6911.
(34) Kido, J.; Kimura, M.; Nagai, K. Multilayer White Light-Emitting Organic Electroluminescent Device. *Science* **1995**, *267*, 1332−1334.
(35) Sun, Y.; Giebink, N. C.; Kanno, H.; Ma, B.; Thompson, M. E.; Forrest, S. R. Management of Singlet and Triplet Excitons for Efficient White Organic Light-Emitting Devices. *Nature* **2006**, *440*, 908−912.
(36) Kamtekar, K. T.; Monkman, A. P.; Bryce, M. R. Recent Advances in White Organic Light-Emitting Materials and Devices (WOLEDs). *Adv. Mater.* **2010**, *22*, 572−578.
(37) Gather, M. C.; Köhnen, A.; Meerholz, K. White Organic Light-Emitting Diodes. *Adv. Mater.* **2011**, *23*, 233−248.
(38) Zang, H.; Shan, X.; Zhou, L.; Lin, P.; Li, R.; Ma, E.; Guo, X.; Du, S. Full-Colour Fluorescent Materials Based on Mixed-Lanthanide(III) Metal−Organic Complexes with High-Efficiency White Light Emission. *J. Mater. Chem. C* **2013**, *1*, 888−891.
(39) Wang, M.-S.; Guo, S.-P.; Li, Y.; Cai, L.-Z.; Zou, J.-P.; Xu, G.; Zhou, W.-W.; Zheng, F.-K.; Guo, G.-C. A Direct White-Light-Emitting Metal−Organic Framework with Tunable Yellow-to-White Photoluminescence by Variation of Excitation Light. *J. Am. Chem. Soc.* **2009**, *131*, 13572−13573.
(40) Ma, X.; Li, X.; Cha, Y.-E.; Jin, L.-P. Highly Thermostable One-Dimensional Lanthanide(III) Coordination Polymers Constructed from Benzimidazole-5,6-dicarboxylic Acid and 1,10-Phenanthroline: Synthesis, Structure, and Tunable White-Light Emission. *Cryst. Growth Des.* **2012**, *12*, 5227−5232.
(41) Ma, M.-L.; Ji, C.; Zang, S.-Q. Syntheses, Structures, Tunable Emission and White Light Emitting Eu^{3+} and Tb^{3+} Doped Lanthanide Metal−Organic Framework Materials. *Dalton Trans.* **2013**, *42*, 10579−10586.
(42) Camposeo, A.; Di Benedetto, F.; Cingolani, R.; Pisignano, D. Full Color Control and White Emission from Conjugated Polymer Nanofibers. *Appl. Phys. Lett.* **2009**, *94*, 043109.
(43) Kotova, O.; Daly, R.; dos Santos, C. M. G.; Boese, M.; Kruger, P. E.; Boland, J. J.; Gunnlaugsson, T. Europium-Directed Self-Assembly of a Luminescent Supramolecular Gel from a Tripodal Terpyridine-Based Ligand. *Angew. Chem., Int. Ed.* **2012**, *51*, 7208−7212.
(44) Hui, J. K.-H.; Yu, Z.; MacLachlan, M. J. Supramolecular Assembly of Zinc Salphen Complexes: Access to Metal-Containing Gels and Nanofibers. *Angew. Chem., Int. Ed.* **2007**, *46*, 7980−7983.
(45) Gavara, R.; Llorca, J.; Lima, J. C.; Rodríguez, L. A Luminescent Hydrogel Based on a New Au(I) Complex. *Chem. Commun.* **2013**, *49*, 72−74.
(46) Strassert, C. A.; Chien, C.-H.; Lopez, M. D. G.; Kourkoulos, D.; Hertel, D.; Meerholz, K.; Cola, L. D. Switching on Luminescence by the Self-Assembly of a Platinum(II) Complex into Gelating Nanofibers and Electroluminescent Films. *Angew. Chem., Int. Ed.* **2011**, *50*, 946−950.
(47) Leong, W. L.; Tam, A. Y.-Y.; Batabyal, S. K.; Koh, L. W.; Kasapis, S.; Yam, V. W.-W.; Vittal, J. J. Fluorescence Enhancement of Coordination Polymeric Gel. *Chem. Commun.* **2008**, 3628−3630.
(48) Tam, A. Y.-Y.; Wong, K. M.-C.; Yam, V. W.-W. Unusual Luminescence Enhancement of Metallogels of Alkynylplatinum(II) 2,6-Bis(*N*-alkylbenzimidazol-2′-yl)pyridine Complexes upon a Gel-to-Sol Phase Transition at Elevated Temperatures. *J. Am. Chem. Soc.* **2009**, *131*, 6253−6260.
(49) Saha, S.; Schön, E.-M.; Cativiela, C.; Díaz, D. D.; Banerjee, R. Proton-Conducting Supramolecular Metallogels from the Lowest Molecular Weight Assembler Ligand: A Quote for Simplicity. *Chem.—Eur. J.* **2013**, *19*, 9562−9568.
(50) Lee, H.; Jung, S. H.; Han, W. S.; Moon, J. H.; Kang, S.; Lee, J. Y.; Jung, J. H.; Shinaki, S. A Chromo-Fluorogenic Tetrazole-Based $CoBr_2$ Coordination Polymer Gel as a Highly Sensitive and Selective Chemosensor for Volatile Gases Containing Chloride. *Chem.—Eur. J.* **2011**, *17*, 2823−2827.
(51) Barman, S.; Garg, J. A.; Blacque, O.; Venkatesan, K.; Berke, H. Triptycene based Luminescent Metal−Organic Gels for Chemosensing. *Chem. Commun.* **2012**, *48*, 11127−11129.
(52) Wu, G.; Wang, X.-F.; Okamura, T.; Sun, W.-Y.; Ueyama, N. Syntheses, Structures and Photoluminescence Properties of Metal(II) Halide Complexes with Pyridine-Containing Flexible Tripodal Ligands. *Inorg. Chem.* **2006**, *45*, 8523−8532.
(53) Wu, G.; Wang, X.-F.; Okamura, T.; Chen, M.; Sun, W.-Y.; Ueyama, N. Syntheses, Structures and Properties of Silver(I) Complexes with Flexible 1,3,5-Tris(pyridylmethoxyl)benzene Ligands. *J. Solid State Chem.* **2010**, *183*, 2174−2182.
(54) Liu, Y.-R.; He, L.; Zhang, J.; Wang, X.; Su, C.-Y. Evolution of Spherical Assemblies to Fibrous Networked Pd(II) Metallogels from a Pyridine-Based Tripodal Ligand and their Catalytic Property. *Chem. Mater.* **2009**, *21*, 557−563.
(55) Xing, B.; Choi, M.-F.; Xu, B. Design of Coordination Polymer Gels as Stable Catalytic Systems. *Chem.—Eur. J.* **2002**, *8*, 5028−5032.
(56) Banerjee, S.; Adarsh, N. N.; Dastidar, P. A Crystal Engineering Rationale in Designing a Cd^{II} Coordination Polymer Based Metallogel Derived From a C3 Symmetric Tris-amide-Tris-carboxylate Ligand. *Soft Matter* **2012**, *8*, 7623−7629.
(57) Samai, S.; Biradha, K. Chemical and Mechano Responsive Metal−Organic Gels of Bis(benzimidazole)-based Ligands with Cd(II) and Cu(II) Halide Salts: Self Sustainability and Gas and Dye Sorptions. *Chem. Mater.* **2012**, *24*, 1165−1173.
(58) Sheldrick, G. M. *SHELX-97, Program for the Solution and Refinement of Crystal Structures*; University of Göttingen: Göttingen, Germany, 1997.
(59) Hamilton, T. D.; Bučar, D.-K.; Baltrusaitis, J.; Flanagan, D. R.; Li, Y.; Ghorai, S.; Tivanski, A. V.; MacGillivray, L. R. Thixotropic Hydrogel Derived from a Product of an Organic Solid-State Synthesis: Properties and Densities of Metal-organic Nanoparticles. *J. Am. Chem. Soc.* **2011**, *133*, 3365−3371.
(60) Gasnier, A.; Royal, G.; Terech, P. Metallo-Supramolecular Gels Based on a Multitopic Cyclam Bis-terpyridine Platform. *Langmuir* **2009**, *25*, 8751−8762.
(61) Larsen, C. B.; van der Salm, H.; Clark, C. A.; Elliott, A. B. S.; Fraser, M. G.; Horvath, R.; Lucas, N. T.; Sun, X.-Z.; George, M. W.; Gordon, K. C. Intraligand Charge-transfer Excited States in Re(I) Complexes with Donor-Substituted Dipyridophenazine Ligands. *Inorg. Chem.* **2014**, *53*, 1339−1354.
(62) Liu, K.; Meng, L.; Mo, S.; Zhang, M.; Mao, Y.; Cao, X.; Huang, C.; Yi, T. Colour Change and Luminescence Enhancement in a Cholesterol-Based Terpyridyl Platinum Metallogel via Sonication. *J. Mater. Chem. C* **2013**, *1*, 1753−1762.
(63) Yong, G.-P.; Zhang, Y.-M.; She, W.-L.; Li, Y.-Z. Stacking-Induced White-Light and Blue-Light Phosphorescence from Purely Organic Radical Materials. *J. Mater. Chem. C* **2011**, *21*, 18520−18522.
(64) Lee, J. H.; Lee, H.; Seo, S.; Seo, M. L.; Kang, S.; Lee, J. Y.; Jung, J. H. Fluorescence Enhancement of a Tetrazole-based Pyridine Coordination Polymer Hydrogel. *New J. Chem.* **2011**, *35*, 1054−1059.
(65) Chaudhari, A. K.; Nagarkar, S. S.; Joarder, B.; Ghosh, S. K. A Continuous π-Stacked Starfish Array of Two-Dimensional Luminescent MOF for Detection of Nitro Explosives. *Cryst. Growth Des.* **2013**, *13*, 3716−3721.

(66) Lan, A.; Li, K.; Wu, H.; Olson, D. H.; Emge, T. J.; Ki, W.; Hong, M.; Li, J. A Luminescent Microporous Metal−Organic Framework for the Fast and Reversible Detection of High Explosives. *Angew.Chem., Int. Ed.* **2009**, *48*, 2334−2338.
(67) Pramanik, S.; Zheng, C.; Zhang, X.; Emge, T. J.; Li, J. New Microporous Metal−Organic Framework Demonstrating Unique Selectivity for Detection of High Explosives and Aromatic Compouds. *J. Am. Chem. Soc.* **2011**, *133*, 4153−4155.
(68) Wang, Y.; La, A.; Ding, Y.; Liu, Y.; Lei, Y. Novel Signal-amplifying Fluorescent Nanofibers for Naked- Eye-Based Ultra-sensitive Detection of Buried Explosives and Explosive Vapors. *Adv. Funct. Mater.* **2012**, *22*, 3547−3555.